Chapter 11

OCT Application Before and After Cataract Surgery

Xiaogang Wang, Jing Dong, Suhua Zhang and Bin Sun

Additional information is available at the end of the chapter

http://dx.doi.org/10.5772/intechopen.77281

Abstract

Optical coherence tomography (OCT), especially anterior segment OCT (AS-OCT), plays an important role in ophthalmology. With the technology evolving from time-domain to spectral-domain, more and more detailed ocular information has become available. Anterior segment OCT provides particularly useful information for cataract surgeons. This chapter focuses mainly on AS-OCT evaluation of eyes before and after cataract surgery. Four aspects including: (1) anterior lens capsule and lens epithelium evaluation using spectral-domain OCT (SD-OCT); (2) investigation of clear corneal incision in femtosecond laser assisted cataract surgery using SD-OCT; (3) capsular block syndrome evaluation before and after treatment using SD-OCT; (4) IOL power calculation in post-myopic excimer laser eyes using SD-OCT, will be discussed in this chapter.

Keywords: OCT, anterior lens capsule, clear corneal incision, capsular block syndrome, Fuchs heterochromic cyclitis, intraocular lens

1. Introduction

Since the introduction of ophthalmic optical coherence tomography (OCT) in 1991, it has been widely used in ophthalmology over the years [1]. The OCT interferometer detects and measures the echo delay time of light, which is projected from a super-luminescent diode and then reflected from different ocular structures. Compared with the 100-μm image resolution of ultrasonography, OCT can, in a non-invasive, non-contact procedure, provide detailed cross-sectional images of the eye on a 10-μm scale. Compared to conventional time-domain anterior segment OCT (AS-OCT) system (1300 nm), a shorter-wavelength infrared light beam (820 nm) is used for the spectral-domain AS-OCT system. This chapter will mainly focus on

anterior segment time-domain and spectral-domain OCT applications before and after cataract surgery. Four aspects will be discussed in this chapter:

- Anterior lens capsule and lens epithelium evaluation in senile cataract and Fuchs' heterochromic cyclitis using spectral-domain anterior segment OCT (SD-OCT);
- Investigation of clear corneal incision in manual phacoemulsification and femtosecond laser assisted cataract surgery using SD-OCT;
- Capsular block syndrome evaluation before and after treatment using SD-OCT;
- IOL power calculation (true net power measurement) in post-myopic excimer laser eyes using SD-OCT.

2. Anterior lens capsule complex measurement using SD-OCT

The lens, as a transparent structure, is a very important refractive element of the human eye. It consists of three major components: capsule, epithelium, and lens substance [2]. The lens epithelial cells and fibers keep the balance of molecules moving into and out of the lens. Previous histological studies have demonstrated that the lens capsule thickness varies by location and that the posterior capsule is the thinnest. The lens epithelium, a single layer of cuboidal cells beneath the anterior capsule, extends to the equatorial lens bow. The lens substance consists of densely packed cells with little extracellular space. With the development of time-domain

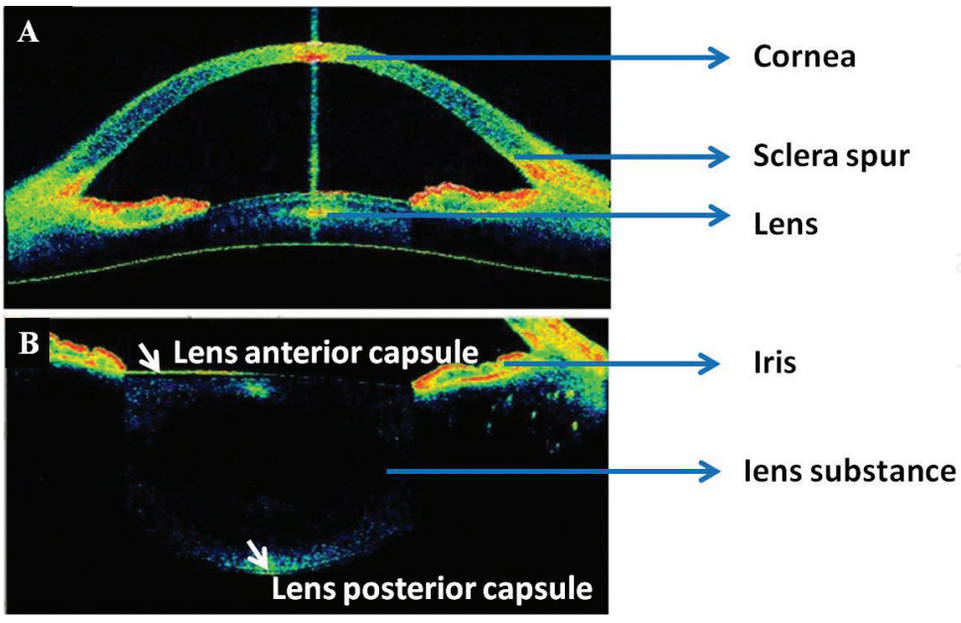

Figure 1. The entire anterior chamber and lens cross-sectional images using OSE-1200 time-domain anterior segment optical coherence tomography (software version 2013.1.1.90; Moptim, Inc., Shenzhen, Guangdong, China). Panel A shows the anterior segment structure: cornea, sclera spur, iris and lens; panel B shows the lens anterior capsule, lens posterior capsule, and lens substance.

OCT, it became possible to image the entire anterior chamber and lens in vivo (**Figure 1**) [3]. Due to the limited resolution (around 15-μm), it was not possible to measure the thickness of the lens capsule or the epithelium.

A previous study manually measured and constructed an anterior lens capsule thickness map across the entire field of view using a femtosecond laser OCT system, which has a central wave length of 780 nm with an axial resolution of 2.3 μm [4]. In a study conducted by Szkulmowski et al., it was reported that the anterior lens capsule and epithelium could be clearly imaged using a SD-OCT system with a central wavelength of 820 nm and axial resolution of 4.2 μm with the help of the speckle contrast reduction technique [5]. The commercial Avanti RTVue XR spectral-domain OCT system provides a high-resolution anterior segment scanning protocol with a scan length of 8 mm and an axial resolution of 5 μm. It can show a substantially clearer delineation after the two highly reflective layers, the anterior lens capsule and the subcapsular epithelium, are combined (**Figure 2**).

We defined the combination of anterior lens capsule and the subcapsular epithelium as the anterior lens capsular complex (ALCC) in a previous study [6]. One hundred thirty-four normal eyes (age range: 5–86 years) were investigated using the Avanti RTVue XR OCT system. The results indicated that the manual measurement of ALCC was both reproducible and reliable. The mean thickness of the central ALCC was approximately 33 μm, which is approximately 15 μm thicker than the anterior lens capsule values calculated using time-domain OCT and other imaging modalities [4, 7]. Therefore, we hypothesized that the subcapsular epithelium was approximately 15 μm thick in vivo. Moreover, a positive correlation between age and ALCC was noted in our study. A 10-year increase in age resulted in a 0.74–1.4 μm increase in the ALCC thickness. From a certain point of view, these findings were consistent

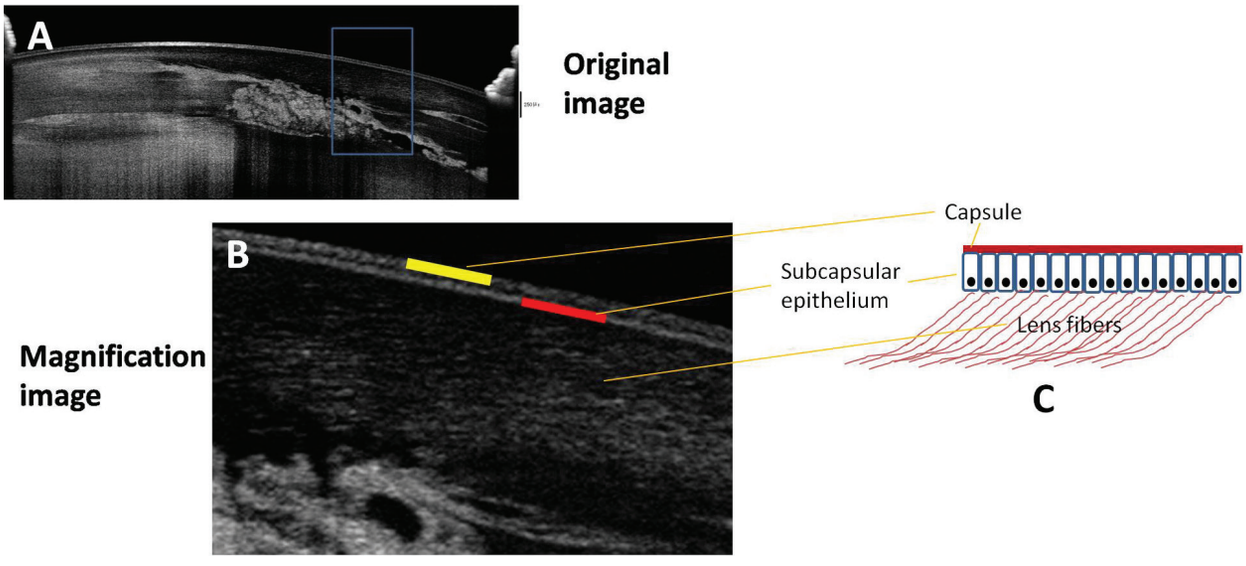

Figure 2. A horizontal anterior segment scanning image of the central part of the lens and the dilated pupil margin in a 34-year-old female using the Avanti RTVue XR spectral-domain optical coherence tomograph (panel A). Panel B shows a magnification of the selected area in panel A (blue frame). Panel C demonstrates the schematic diagram of the anterior lens capsule (corresponding to the yellow reflective layer in panel B), the subcapsular epithelium (corresponding to the red reflective layer in panel B), and the lens fibers.

with previous findings regarding the positive correlation between age and lens capsule or total lens thickness [8, 9].

With the help of anterior segment SD-OCT, researchers also can obtain more detailed useful information regarding accommodation, presbyopia, Fuchs' heterochromic iridocyclitis (**Figure 3**), posterior capsule opacification, and pseudoexfoliation syndrome [10–13]. Moreover, with the OCT technology development, the respective measurement of anterior capsule, posterior capsule and epithelium layer thickness, even plotting corresponding topography in specific regions will be available in the future.

2.1. Summary

In summary, anterior segment SD-OCT can be used to visualize anterior and posterior lens capsule, lens epithelium, keratic precipitates, iris stroma atrophy. The use of anterior segment SD-OCT will enable us to better investigate changes in lens structure of patients with Fuchs' heterochromic iridocyclitis or other lens related conditions.

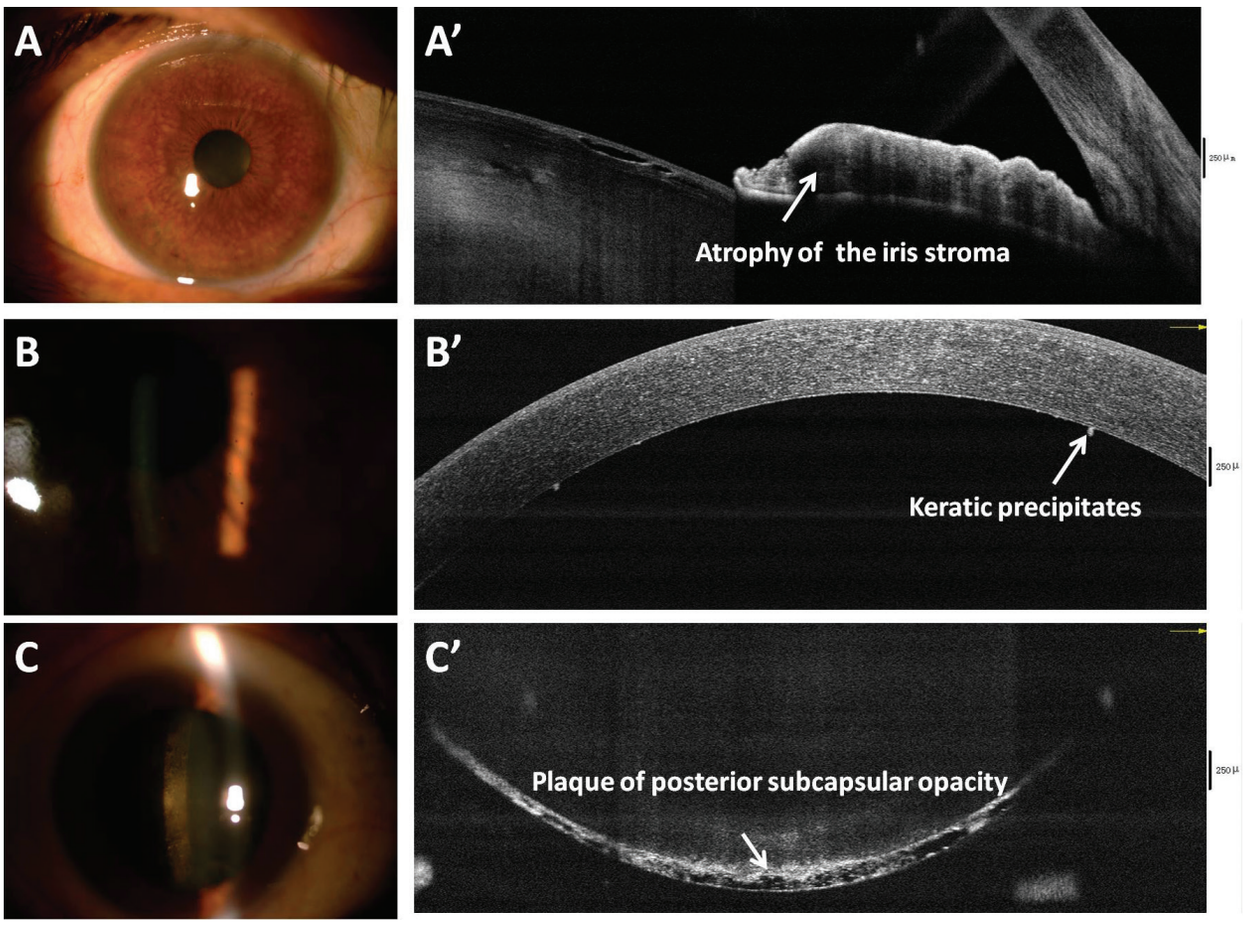

Figure 3. Color images and optical coherence tomography cross-sectional images of a 60-year-old female with Fuchs' heterochromic iridocyclitis. The anterior color slit-lamp photos and corresponding anterior segment OCT cross-sectional images show atrophy of the iris stroma (panel A, A'), small keratic precipitates scattered over the entire corneal endothelium (panel B, B'), and plaque of posterior subcapsular opacity (panel C, C').

3. Investigation of clear corneal incision using SD-OCT

In most industrialized countries, cataract surgery accounts for the largest proportion of surgical interventions in ophthalmology. The advent of minimal incision, phacoemulsification (introduced by Charles Kelman in the 1970s), and foldable intraocular lens, has made cataract surgery safer and more efficient [14]. Moreover, modern cataract surgery combined with new generation intraocular lens types, which can be designated refractive surgery, aims to provide optimal visual quality and render the visual function better [15]. As a significant part of the cataract surgery, the constructional architecture of proper clear corneal incisions (CCIs) is vital for a perfect outcome of phacoemulsification. Faulty CCI construction can lead to complications, such as wound leak, Descemet's membrane detachment, and excessive surgically-induced astigmatism, and is a situation every cataract surgeon attempts to avoid. However, it is not easy to predictably construct perfect manual single-plane, two-plane, or three-plane clear corneal tunnels using steel or diamond blades [16]. With the higher expectations of patients from modern cataract and refractive surgery and the advent of trifocal and accommodating IOLs, femtosecond laser was introduced into cataract surgery by Zoltan Nagy in 2009 [17]. Previous studies demonstrated that a femtosecond laser-assisted cataract surgery technique could provide repeatable, predictable clear corneal incisions, perfect capsulotomies, and safe nuclear fragmentation [18, 19]. Therefore, CCIs created using femtosecond laser have the advantage of predictable configuration and dimensions.

Clinical manual CCI parameters (incision location, angle of incision, incision length) and features (posterior wound gape, Descemet's membrane detachment, posterior wound retraction, loss of coaptation along the CCI tunnel) in the early postoperative period (up to 1 month) of standard cataract surgery have been reported [20–23]. Based on the above-mentioned studies, we evaluated the quantitative CCI parameters and features in subjects who underwent femtosecond laser-assisted cataract surgery [24]. Except for no sign of loss of coaptation along the CCI tunnel, all the other three CCI features were found in femtosecond laser CCI (**Figure 4**).

As expected, the femtosecond laser lens fragmentation ensures that the phacoemulsification energy (Femto group: 16 ± 13%; manual group: 20 ± 5%) and effective phacoemulsification time (Femto group: 17 ± 9 s; manual group: 32 ± 13 s) were dramatically lower in the Femto group than in the conventional manual group. Moreover, the femtosecond laser group had a lower incidence of Descemet's membrane detachment and posterior wound gape at each follow-up time-point. However, a higher incidence of posterior wound retraction was found in the femtosecond laser group.

Descemet's membrane detachment may potentially hinder the local endothelium pump mechanism and affect corneal wound healing. The routine procedure for CCI by femtosecond laser is from the anterior chamber (inner cornea) to the epithelium (outer cornea), which makes the Descemet's membrane detachment an unusual complication for this group. However, phacoemulsification probe manipulation through the CCI, the blunt dissection of the tunnel, and incision hydration probably contributed to the occurrence of Descemet's membrane detachment in the femtosecond group. For the difference in posterior wound gape incidence, we are inclined to implicate the difference in tunnel incision geometry between the

two groups. Compared to 1-plane manual CCI, we mainly used a 2-plane CCI in femtosecond group. As previous studies have mentioned, a 2-plane CCI with a partial lamellar cut positioned parallel to the collagen lamellae may improve the shearing force effects of the stromal collagen lamellae across the entire depth of the cornea [25–27]. Posterior wound retraction, defined as an abrupt step-off or recession of the central edge of the posterior wound surface, was not observed in manual group in this study. This may be attributed to the relatively high incidence of posterior wound gape, in which the posterior wound margins were still separated. A high incidence of posterior wound retraction in the femtosecond group may indicate remodeling of the CCI resulting from endothelial cell necrosis, molecular dissociation, and biomechanical and thermal changes from the femtosecond laser [28]. A previous study, using transmission electron microscopy confirmed the difference between femtosecond laser corneal flap formation (necrotic keratocytes) and microkeratome corneal flap formation (keratocyte apoptosis), which may potentially explain the different incidence of posterior wound retraction in this study [29]. Moreover, the above-mentioned three CCI features may cause changes to posterior corneal curvature, corneal astigmatism, and total corneal power; these should be evaluated in future studies.

3.1. Summary

Anterior segment SD-OCT can highlight CCIs findings that are not as obvious by UBM, slit lamp. The ability to detect detailed postoperative corneal incision changes of standard or femtosecond laser-assisted cataract surgery is clinically important as it allows for the evaluation

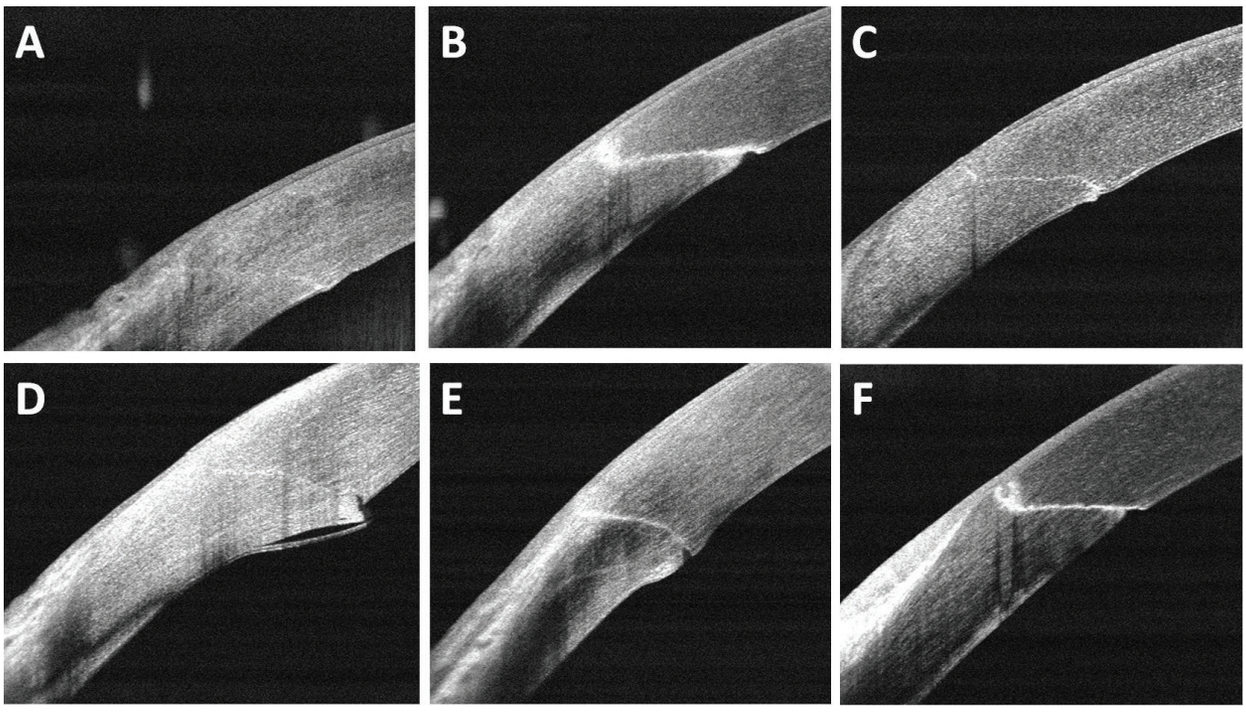

Figure 4. High-resolution anterior segment SD-OCT clear corneal incision images of femtosecond laser-assisted cataract surgery showing a 1-plane CCI (panel A), 2-plane CCI (panel B), 3-plane CCI (panel C), stripping of Descemet's membrane (panel D), posterior wound gape (panel E), and posterior wound retraction (panel F).

and comparison of surgical induced astigmatism and corneal remodeling by different surgical technology. In the future, clear corneal incision length, inner and outer corneal incision thickness, even the lens capsulotomy margin may be evaluated in traditional and femtosecond laser-assisted cataract surgery using OCT.

4. Capsular block syndrome evaluation before and after treatment using SD-OCT

Capsular block syndrome (CBS), as an uncommon complication of phacoemulsification, is characterized by the accumulation of liquid between the IOL and posterior capsule [30]. Davison and Holtz first described this syndrome in 1990 and 1992, respectively [31, 32]. In

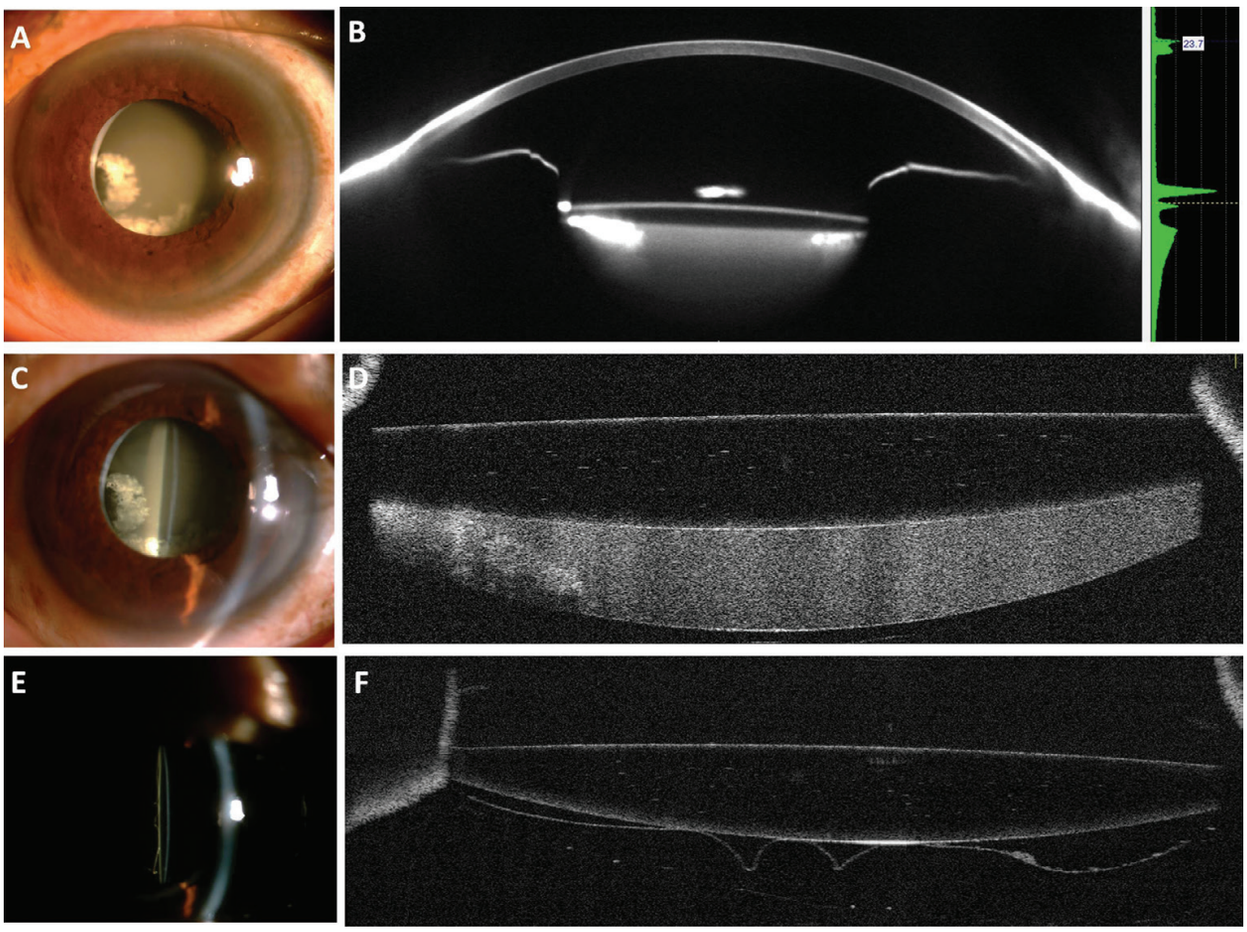

Figure 5. Slit lamp, Pentacam Scheimpflug, and AS-OCT images of an ultra-late capsular block syndrome before (panels A–D) and after surgery (panels E and F). Slit lamp photograph shows white proliferation tissue infero-nasally and nasal tight adhesion of anterior capsule opening fibrosis and IOL (panel A). Scheimpflug-based photography showing the contour of the IOL and the underlying milky-white fluid (panel B). Slit lamp photograph showing a large amount of white fluid trapped behind the IOL (panel C). AS-OCT showing a transparent IOL and accumulation of a milky-white liquefied substance between the posterior capsular bag and IOL (panel D). Slit lamp photograph showing posterior capsular folds and no milky-white liquid after surgery (panel E). AS-OCT shows that the capsular block syndrome is resolved after surgery, with parts of posterior capsule in contact with IOL and posterior capsule folds (panel F).

1993, Masket first used the term CBS to refer to this condition [33]. Due to a continuous capsulorhexis and adhesion of anterior capsule to the IOL, the exchange of aqueous between the anterior chamber and inner capsular bag gets blocked and fluid is retained behind the IOL [34]. Generally, CBS is related to IOL implantation in the capsular bag, but it has also be reported in cases with IOL implantation in the sulcus [35, 36]. Various manifestations of CBS, such as decreased visual acuity, ocular hypertension, closed angle glaucoma, and posterior capsule rupture have been reported. The two main reasons for vision loss include: (1) the effective position of IOL moves forward (myopic shift); (2) a white liquid accumulates behind the IOL (lacteocrumenasia) [30]. Based on time to development, CBS can be divided into three types: intraoperative capsular block, early postoperative CBS, and late postoperative CBS [37, 38]. Most intraoperative CBS occurs due to hydrodissection maneuvers in posterior polar or white cataract surgeries. Due to the block of capsulorhexis borders, liquid accumulates between the posterior nucleus and the posterior capsule. Increasing pressure in the capsular bag may cause posterior capsular rupture and even lens luxation into the vitreous [38]. Early postoperative CBS occurs 1–15 days after cataract surgery. The two main causes are as follows: (1) viscoelastic accumulation behind the IOL; (2) osmotic gradient behind the IOL induced by viscoelastic materials or trapped lens fragments [38, 39]. On average, late postoperative CBS occurs approximately 3.8 years after cataract surgery and deposition of a white fluid (proliferation and pseudo-metaplasia of the lens epithelium) is found between the IOL and posterior capsular bag [34, 40].

A simple, clinical examination can diagnose most CBS cases. With the development of ophthalmic imaging technology t, a definitive diagnosis can be achieved using Scheimpflug-based photography, AS-OCT, or anterior segment UBM. Compared with Scheimpflug-based photography, spectral domain AS-OCT fails to provide complete anterior chamber information but it can provide more details about the IOL and any fluid between the IOL and posterior capsular bag (**Figure 5**).

In some CBS cases with relatively transparent fluid behind the IOL and a large distance between IOL and posterior capsule, UBM, Scheimpflug-based photography or AS-OCT can just demonstrate a partial cross-sectional image (**Figure 6**).

Compared to surgical management, we may also choose anterior or posterior capsulotomy with a Nd:YAG laser to treat CBS, especially for early postoperative and non-cellular late postoperative cases [41]. Due to the relatively lower success rate and higher recurrence rate for anterior capsulotomy, some doctors may choose posterior capsulotomy [42]. In some cases, posterior capsulotomy may cause unexpected irregular posterior capsule rupture, which may cause the IOL to drop into the vitreous cavity (**Figure 7**). Therefore, surgical management is a better choice for late CBS, especially incases with dense white liquid, which makes aiming the Nd:YAG laser accurately almost impossible, and the capsulotomy may cause IOP increase or vitreous inflammation [43]. As an important imaging technology, with the imaging depth enhanced, more and more details about CBS and other posterior capsular related disease can be investigated using OCT.

4.1. Summary

While varying in cause and course, these CBS cases all consistently demonstrated the ability of anterior segment SD-OCT to clearly diagnose and delineate with impressive detail the onset

and treatment follow-up. Anterior segment SD-OCT offers extraordinary anatomic details, the more accurate diagnosis, and the potential of quantitative measurement to improve the assessment of treatment efficacy.

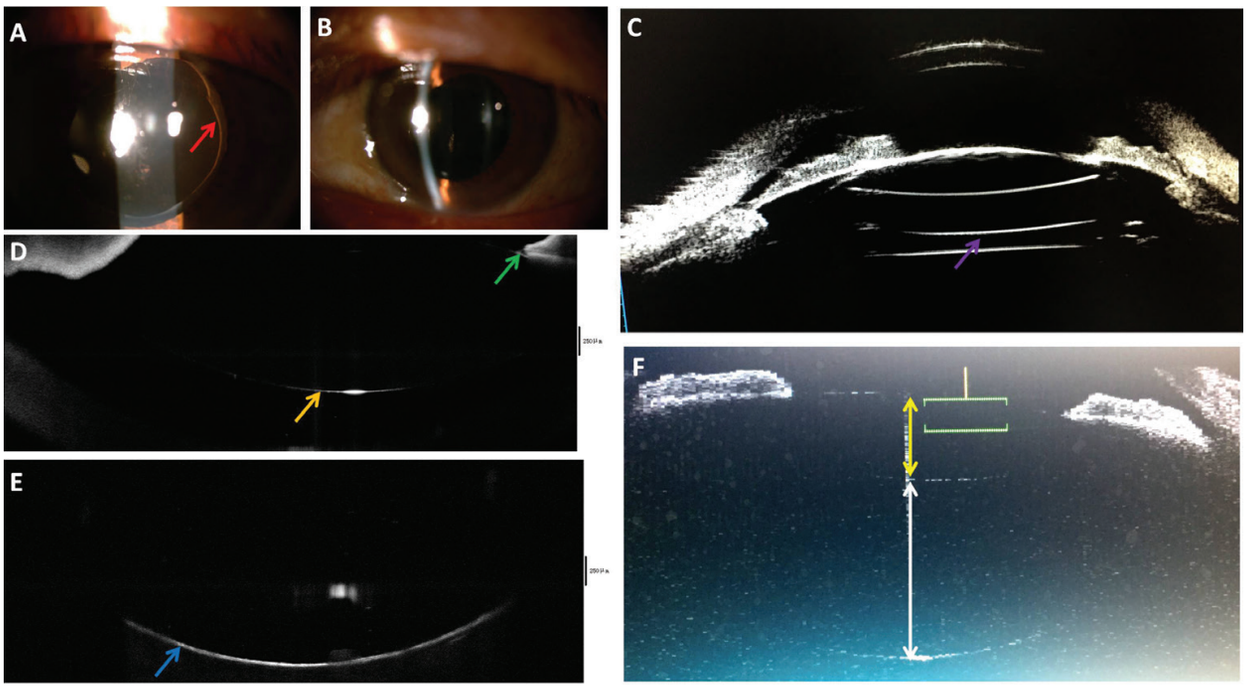

Figure 6. Slit lamp, UBM, and AS-OCT images of a late postoperative capsular block syndrome before Nd:YAG laser treatment. Slit lamp photograph showing capsulorhexis edge (red arrow), anterior IOL optic tightly in contact with the entire anterior capsule (panel A). Slit-lamp biomicroscopy showing transparent fluid behind the IOL (panel B). Due to the limited imaging penetration, UBM image showing artifacts (purple arrow) but not the posterior capsule (panel C). Due to limited imaging depth, spectral-domain AS-OCT fails to show posterior IOL surface (orange arrow), tight adhesion between anterior IOL surface and capsulorhexis edge (green arrow), and posterior capsule (panel E, blue arrow) in one cross-sectional image (panels D and E). Time-domain AS-OCT showing IOL thickness around 1.5 mm (yellow line segment) and the distance between IOL and posterior capsule of about 3.1 mm (white line segment) in one cross-sectional image (panel F).

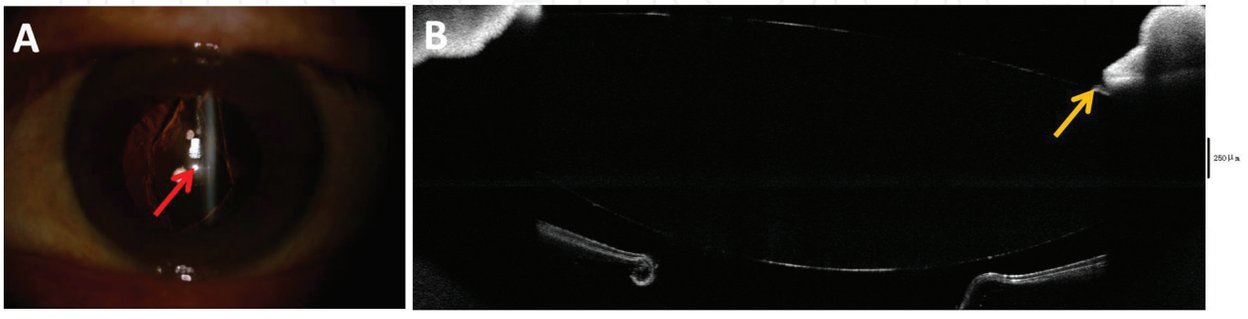

Figure 7. Slit-lamp and AS-OCT images of a late postoperative capsular block syndrome after Nd:YAG laser treatment. Slit-lamp photograph shows irregular posterior capsule rupture (red arrow) after ND:YAG laser treatment (panel A). Spectral-domain AS-OCT cross-sectional image showing posterior capsule breaks with capsular edge rolling and significant decrease in the distance between the IOL and posterior capsule (compared to **Figure 6** panel F). The tight adhesion between anterior IOL surface and anterior capsulorhexis edge (yellow arrow) may prevent the IOL from falling into the vitreous cavity through the big posterior capsule rupture (panel B).

5. IOL power calculation in post-myopic excimer laser eyes using SD-OCT

It is well known that correct IOL power calculation in patients undergoing cataract surgery depends mainly on the accurate measurement of corneal power, axial length, corneal keratometry, and the effective lens position after surgery [44, 45]. Due to index of refraction error, instrument error, and IOL formula error, precise prediction of IOL power is always a big challenge for cataract surgery in patients with previous corneal refractive surgery (PRK, LASIK, RK) [46–51]. For post corneal refractive surgery cataract patients, both, patient expectations of spectacle independence and reduction in the accuracy of conventional IOL power calculation formulas due to previous corneal surgery should be considered. To deal with these issues, many innovative post-corneal refractive surgery IOL power calculation formulas have been developed [52–58]. Compared to traditional keratometry, RTVue spectral-domain AS-OCT can measure anterior and posterior corneal curvature and then calculate the net corneal power, which in conjunction with IOLMaster biometry data (AL, ACD) provides the IOL power [59]. Previous studies have demonstrated that Fourier-domain AS-OCT can provide highly repeatable corneal power measurement and spectral-domain OCT-based IOL formulas have also provided promising results in post-refractive surgery IOL calculation in eyes undergoing cataract surgery; this is especially meaningful for patients for whom prior data are not available [59–61]. To avoid significant IOL power fluctuation between different formulas, surgeons can also use ASCRS online post-refractive IOL calculator (link: http://iolcalc.ascrs.org/) to get the average IOL power value to make sure the real postoperative refraction deviation from the target refraction is not large (**Figure 8**).

5.1. Summary

Anterior segment SD-OCT can noncontactly provide true net corneal power, which is essential for IOL power calculation after excimer laser corneal surgery. The SD-OCT-based IOL formulas enable to provide promising results in post-refractive surgery IOL calculation, especially meaningful for eyes whose prior data unavailable.

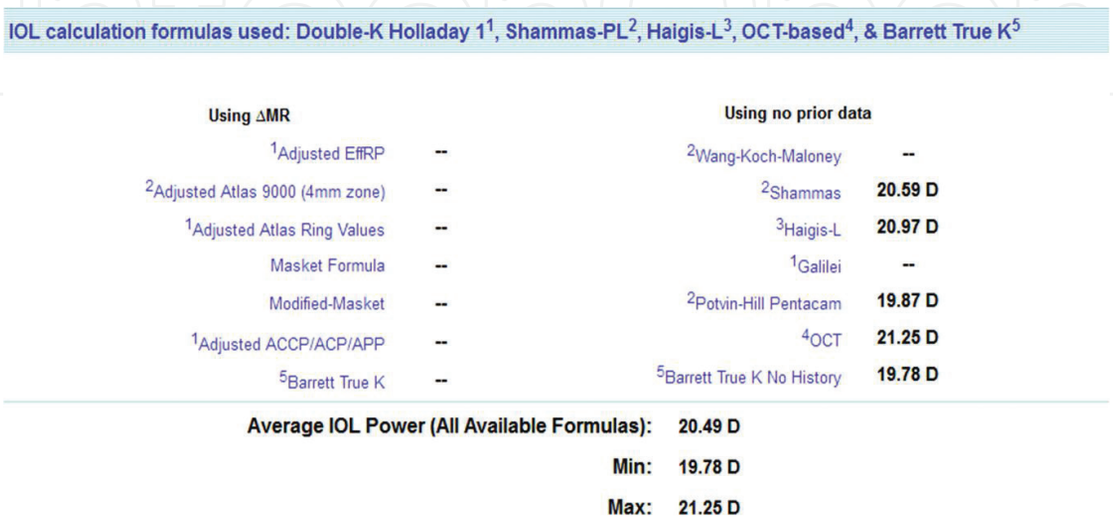

Figure 8. Average IOL power information for all available formulas using ASCRS online post-refractive IOL calculator.

6. Conclusions

In conclusion, OCT, as a noninvasive and high-resolution imaging technology, can provide the ophthalmologist with clinically useful findings not only about the retina, but also for the cornea, lens, and anterior chamber. Anterior segment high-speed SD-OCT system offers efficient information about lens capsule evaluation, clear corneal incision investigation, capsular block syndrome management, and post-refractive surgery IOL power calculation. In the future, anterior segment SD-OCT may be a useful tool for detecting and monitoring more ocular disease progression and treatment response in clinic.

Grant information

This work was supported by the National Natural Science Foundation of China under Grant No. 81501544.

Financial interests

The authors have neither a conflict of interest nor commercial interest in the equipment mentioned in this paper.

Author details

Xiaogang Wang[1]*, Jing Dong[2], Suhua Zhang[1] and Bin Sun[1]

*Address all correspondence to: movie6521@163.com

1 Department of Cataract, Shanxi Eye Hospital, Taiyuan, China

2 Department of Ophthalmology, The First Hospital of Shanxi Medical University, Shanxi, PR China

References

[1] Huang D, Swanson EA, Lin CP, Schuman JS, Stinson WG, Chang W, Hee MR, Flotte T, Gregory K, Puliafito CA, et al. Optical coherence tomography. Science. 1991;**254**:1178-1181

[2] Seland JH. Ultrastructural changes in the normal human lens capsule from birth to old age. Acta Ophthalmologica. 1974;**52**:688-706

[3] Radhakrishnan S, Rollins AM, Roth JE, Yazdanfar S, Westphal V, Bardenstein DS, Izatt JA. Real-time optical coherence tomography of the anterior segment at 1310 nm. Archives of Ophthalmology. 2001;**119**:1179-1185

[4] Kaluzny BJ, Gora M, Karnowski K, Grulkowski I, Kowalczyk A, Wojtkowski M. Imaging of the lens capsule with an ultrahigh-resolution spectral optical coherence tomography prototype based on a femtosecond laser. The British Journal of Ophthalmology. 2010;**94**:275-277

[5] Szkulmowski M, Gorczynska I, Szlag D, Sylwestrzak M, Kowalczyk A, Wojtkowski M. Efficient reduction of speckle noise in optical coherence tomography. Optics Express. 2012;**20**:1337-1359

[6] Dong J, Jia Y, Zhang Y, Zhang H, Jia Z, Zhang S, Wu Q, Hu Q, Zhang T, Wang X. Anterior lens capsule and epithelium thickness measurements using spectral-domain optical coherence tomography. BMC Ophthalmology. 2017;**17**:94

[7] Hawlina M, Stunf S, Hvala A. Ultrastructure of anterior lens capsule of intumescent white cataract. Acta Ophthalmologica. 2011;**89**:e367-e370

[8] Zeng Y, Liu X, Wang T, Zhong Y, Huang J, He M. Correlation between lens thickness and central anterior chamber depth. Eye Science. 2012;**27**:124-126

[9] Barraquer RI, Michael R, Abreu R, Lamarca J, Tresserra F. Human lens capsule thickness as a function of age and location along the sagittal lens perimeter. Investigative Ophthalmology & Visual Science. 2006;**47**:2053-2060

[10] Farouk MM, Naito T, Shinomiya K, Eguchi H, Sayed KM, Nagasawa T, Katome T, Mitamura Y. Optical coherence tomography reveals new insights into the accommodation mechanism. Journal of Ophthalmology. 2015;**2015**:510459

[11] Kim E, Ehrmann K, Uhlhorn S, Borja D, Arrieta-Quintero E, Parel JM. Semiautomated analysis of optical coherence tomography crystalline lens images under simulated accommodation. Journal of Biomedical Optics. 2011;**16**:056003

[12] Kaluzny BJ, Szkulmowska A, Kaluzny JJ, Bajraszewski T, Szkulmowski M, Kowalczyk A, Wojtkowski M. In vivo imaging of posterior capsule opacification using spectral optical coherence tomography. Journal of Cataract and Refractive Surgery. 2006;**32**:1892-1895

[13] Zheng X, Sakai H, Goto T, Namiguchi K, Mizoue S, Shiraishi A, Sawaguchi S, Ohashi Y. Anterior segment optical coherence tomography analysis of clinically unilateral pseudoexfoliation syndrome: Evidence of bilateral involvement and morphologic factors related to asymmetry. Investigative Ophthalmology & Visual Science. 2011;**52**:5679-5684

[14] Pandey SK, Milverton EJ, Maloof AJ. A tribute to Charles David Kelman MD: Ophthalmologist, inventor and pioneer of phacoemulsification surgery. Clinical & Experimental Ophthalmology. 2004;**32**:529-533

[15] Saraiva J, Neatrour K, Waring Iv GO. Emerging technology in refractive cataract surgery. Journal of Ophthalmology. 2016;**2016**:7309283

[16] Calladine D, Ward M, Packard R. Adherent ocular bandage for clear corneal incisions used in cataract surgery. Journal of Cataract and Refractive Surgery. 2010;**36**:1839-1848

[17] Nagy Z, Takacs A, Filkorn T, Sarayba M. Initial clinical evaluation of an intraocular femtosecond laser in cataract surgery. Journal of Refractive Surgery. 2009;**25**:1053-1060

[18] Bissen-Miyajima H, Hirasawa M, Nakamura K, Ota Y, Minami K. Safety and reliability of femtosecond laser-assisted cataract surgery for Japanese eyes. Japanese Journal of Ophthalmology. 2018;**62**:226-230

[19] Agarwal A, Jacob S. Current and effective advantages of femto phacoemulsification. Current Opinion in Ophthalmology. 2017;**28**:49-57

[20] Fine IH, Hoffman RS, Packer M. Profile of clear corneal cataract incisions demonstrated by ocular coherence tomography. Journal of Cataract and Refractive Surgery. 2007;**33**:94-97

[21] Schallhorn JM, Tang M, Li Y, Song JC, Huang D. Optical coherence tomography of clear corneal incisions for cataract surgery. Journal of Cataract and Refractive Surgery. 2008;**34**:1561-1565

[22] Wang L, Dixit L, Weikert MP, Jenkins RB, Koch DD. Healing changes in clear corneal cataract incisions evaluated using Fourier-domain optical coherence tomography. Journal of Cataract and Refractive Surgery. 2012;**38**:660-665

[23] Calladine D, Packard R. Clear corneal incision architecture in the immediate postoperative period evaluated using optical coherence tomography. Journal of Cataract and Refractive Surgery. 2007;**33**:1429-1435

[24] Wang X, Zhang Z, Li X, Xie L, Zhang H, Koch DD, Wang L, Zhang S. Evaluation of femtosecond laser versus manual clear corneal incisions in cataract surgery using spectral-domain optical coherence tomography. Journal of Refractive Surgery. 2018;**34**:17-22

[25] Smolek MK, McCarey BE. Interlamellar adhesive strength in human eyebank corneas. Investigative Ophthalmology & Visual Science. 1990;**31**:1087-1095

[26] Shin TJ, Vito RP, Johnson LW, McCarey BE. The distribution of strain in the human cornea. Journal of Biomechanics. 1997;**30**:497-503

[27] Serrao S, Lombardo G, Schiano-Lomoriello D, Ducoli P, Rosati M, Lombardo M. Effect of femtosecond laser-created clear corneal incision on corneal topography. Journal of Cataract and Refractive Surgery. 2014;**40**:531-537

[28] Schultz T, Tischoff I, Ezeanosike E, Dick HB. Histological sections of corneal incisions in OCT-guided femtosecond laser cataract surgery. Journal of Refractive Surgery. 2013;**29**:863-864

[29] Santhiago MR, Wilson SE. Cellular effects after laser in situ keratomileusis flap formation with femtosecond lasers: A review. Cornea. 2012;**31**:198-205

[30] Velez M, Velasquez LF, Rojas S, Montoya L, Zuluaga K, Balparda K. Capsular block syndrome: A case report and literature review. Clinical Ophthalmology. 2014;**8**:1507-1513

[31] Davison JA. Capsular bag distension after endophacoemulsification and posterior chamber intraocular lens implantation. Journal of Cataract and Refractive Surgery. 1990;**16**:99-108

[32] Holtz SJ. Postoperative capsular bag distension. Journal of Cataract and Refractive Surgery. 1992;**18**:310-317

[33] Masket S. Postoperative complications of capsulorhexis. Journal of Cataract and Refractive Surgery. 1993;**19**:721-724

[34] Miyake K, Ota I, Miyake S, Horiguchi M. Liquefied aftercataract: A complication of continuous curvilinear capsulorhexis and intraocular lens implantation in the lens capsule. American Journal of Ophthalmology. 1998;**125**:429-435

[35] Basti S, Nayak H, Mathur U. Capsular bag distension after optic capture of a sulcus-fixated intraocular lens. Journal of Cataract and Refractive Surgery. 1999;**25**:293-295

[36] Durak I, Ozbek Z, Ferliel ST, Oner FH, Soylev M. Early postoperative capsular block syndrome. Journal of Cataract and Refractive Surgery. 2001;**27**:555-559

[37] Kim HK, Shin JP. Capsular block syndrome after cataract surgery: Clinical analysis and classification. Journal of Cataract and Refractive Surgery. 2008;**34**:357-363

[38] Miyake K, Ota I, Ichihashi S, Miyake S, Tanaka Y, Terasaki H. New classification of capsular block syndrome. Journal of Cataract and Refractive Surgery. 1998;**24**:1230-1234

[39] Sugiura T, Miyauchi S, Eguchi S, Obata H, Nanba H, Fujino Y, Masuda K, Akura J. Analysis of liquid accumulated in the distended capsular bag in early postoperative capsular block syndrome. Journal of Cataract and Refractive Surgery. 2000;**26**:420-425

[40] Eifrig DE. Capsulorhexis-related lacteocrumenasia. Journal of Cataract and Refractive Surgery. 1997;**23**:450-454

[41] Pinsard L, Rougier MB, Colin J. Neodymium:YAG laser treatment of late capsular block syndrome. Journal of Cataract and Refractive Surgery. 2011;**37**:2079-2080

[42] Colakoglu A, Kucukakyuz N, Topcuoglu IE, Akar S. Intraocular pressure rise and recurrence of capsular block syndrome after neodymium:YAG laser anterior capsulotomy. Journal of Cataract and Refractive Surgery. 2007;**33**:1344-1346

[43] Qu J, Bao Y, Li M, Zhao M, Li X. Surgical management of late capsular block syndrome. Journal of Cataract and Refractive Surgery. 2010;**36**:1687-1691

[44] Findl O. Biometry and intraocular lens power calculation. Current Opinion in Ophthalmology. 2005;**16**:61-64

[45] Olsen T. Calculation of intraocular lens power: A review. Acta Ophthalmologica Scandinavica. 2007;**85**:472-485

[46] Hoffer KJ. Intraocular lens power calculation after previous laser refractive surgery. Journal of Cataract and Refractive Surgery. 2009;**35**:759-765

[47] Rosa N, Capasso L, Lanza M, Iaccarino G, Romano A. Reliability of a new correcting factor in calculating intraocular lens power after refractive corneal surgery. Journal of Cataract and Refractive Surgery. 2005;**31**:1020-1024

[48] Shammas HJ, Shammas MC. No-history method of intraocular lens power calculation for cataract surgery after myopic laser in situ keratomileusis. Journal of Cataract and Refractive Surgery. 2007;**33**:31-36

[49] Rosa N, De Bernardo M, Borrelli M, Lanza M. New factor to improve reliability of the clinical history method for intraocular lens power calculation after refractive surgery. Journal of Cataract and Refractive Surgery. 2010;**36**:2123-2128

[50] Abulafia A, Hill WE, Koch DD, Wang L, Barrett GD. Accuracy of the Barrett True-K formula for intraocular lens power prediction after laser in situ keratomileusis or photorefractive keratectomy for myopia. Journal of Cataract and Refractive Surgery. 2016;**42**:363-369

[51] Alio JL, Abdelghany AA, Fernandez-Buenaga R. Management of residual refractive error after cataract surgery. Current Opinion in Ophthalmology. 2014;**25**:291-297

[52] Aramberri J. Intraocular lens power calculation after corneal refractive surgery: Double-K method. Journal of Cataract and Refractive Surgery. 2003;**29**:2063-2068

[53] Saiki M, Negishi K, Kato N, Ogino R, Arai H, Toda I, Dogru M, Tsubota K. Modified double-K method for intraocular lens power calculation after excimer laser corneal refractive surgery. Journal of Cataract and Refractive Surgery. 2013;**39**:556-562

[54] Feiz V, Mannis MJ, Garcia-Ferrer F, Kandavel G, Darlington JK, Kim E, Caspar J, Wang JL, Wang W. Intraocular lens power calculation after laser in situ keratomileusis for myopia and hyperopia: A standardized approach. Cornea. 2001;**20**:792-797

[55] Latkany RA, Chokshi AR, Speaker MG, Abramson J, Soloway BD, Yu G. Intraocular lens calculations after refractive surgery. Journal of Cataract and Refractive Surgery. 2005;**31**:562-570

[56] Savini G, Barboni P, Zanini M. Intraocular lens power calculation after myopic refractive surgery: Theoretical comparison of different methods. Ophthalmology. 2006;**113**: 1271-1282

[57] Borasio E, Stevens J, Smith GT. Estimation of true corneal power after keratorefractive surgery in eyes requiring cataract surgery: BESSt formula. Journal of Cataract and Refractive Surgery. 2006;**32**:2004-2014

[58] Haigis W. Intraocular lens calculation after refractive surgery for myopia: Haigis-L formula. Journal of Cataract and Refractive Surgery. 2008;**34**:1658-1663

[59] Fram NR, Masket S, Wang L. Comparison of intraoperative aberrometry, OCT-based IOL formula, Haigis-L, and Masket formulae for IOL power calculation after laser vision correction. Ophthalmology. 2015;**122**:1096-1101

[60] Tang M, Chen A, Li Y, Huang D. Corneal power measurement with Fourier-domain optical coherence tomography. Journal of Cataract and Refractive Surgery. 2010;**36**:2115-2122

[61] Wang Q, Hua Y, Savini G, Chen H, Bao F, Lin S, Lu W, Huang J. Corneal power measurement obtained by Fourier-domain optical coherence tomography: Repeatability, reproducibility, and comparison with Scheimpflug and automated keratometry measurements. Cornea. 2015;**34**:1266-1271

IntechOpen